Thalassas: An International Journal of Marine Sciences (2018) 34:459–469
https://doi.org/10.1007/s41208-018-0093-y

Measuring Method of Solid-Liquid Two-Phase Flow in Slurry Pipeline for Deep-Sea Mining

Hengling Yang [1,2,3] • Shaojun Liu [1,2,3]

Received: 25 July 2017 / Published online: 11 July 2018

Abstract

In order to reduce the influence of fluid noise on the measurement of solid-liquid two-phase flow in slurry pipeline for deep-sea mining, the technique of virtual inductance is introduced to traditional capacitively coupled contactless conductivity detection (C^4D), a measuring method for solid-liquid two-phase flow based on differential C^4D is proposed, and the structure of differential C^4D based on three electrodes is designed. The measuring device was verified in conductive fluid channels at different salinity. The results demonstrated that the amplitude of output voltage of the measuring device decreased obviously with the increase of the salinity of the fluid, and linearly associated with the size and volume concentration of the polymetallic nodules. Virtual inductance could reduce the requirement of C^4D sensor for the excitation power. The measuring device had less noise of output signal and high accuracy. When the KCl solution containing salinity is at the average salinity of seawater 3.5% and the particle size of polymetallic nodules is from 0 to 25 mm, the output voltage increased from 0 to 87 mv. The maximum relative error in two-phase flow velocity measurement is 5.2%, which showed that the measuring method for two-phase flow in the slurry pipeline based on the differential C^4D is effective.

Keywords Deep-sea mining · Two-phase flow · Measuring techniques · Capacitively coupled contactless conductivity detection (C^4D)

Introduction

The ocean is not only rich in oil and gas resources but also has abundant metal mineral resources, such as nickel, copper, cobalt, manganese, and gold. The reserves of some mineral resources in the ocean are tens to several thousand times corresponding to reserves of land. These metal mineral resources in the form of polymetallic nodules and polymetallic sulfides are located at thousands of meters below the seabed (Xiao et al. 2014). Deep-sea mining capacity depends on the development of mining equipment which can adapt to extremely harsh operating environment of deep-sea. Among the three major existing deep-sea mining systems, the pipe-lifting system is the most application potential, as shown in Fig. 1. This system mainly consisted of a collector, soft pipe, middle bin, riser pipe, lifting motor pump, and mining vessel (Liu et al. 2014).

The structure of the collector is shown in Fig. 2. In order to improve the cutting efficiency and reduce the mining pollution, the collector adopted the integrated working method of combining and cutting mineral nodules (Liu et al. 2016).

The structure of the lifting motor pump is shown in Fig. 3. It is a kind of a slurry pump; in addition, it must meet the performance of anti-high pressure, non-blocking, high lift, wear and corrosion resistance, and good reliability.

Fluid transported in deep-sea slurry pipeline is a solid-liquid two-phase flow. Its parameters' accurate measurement is directly related to the stability and economic operation of deep-sea mining system.

The measurement of multiphase flow parameters was a difficult problem, which was urgently to be solved in industrial. At present, due to the physical properties of multiphase fluid and the mechanisms of flow process complex, there was not a single measuring method that can fully adapt to various multiphase flows. With the development of science and

✉ Hengling Yang
65065325@qq.com

✉ Shaojun Liu
153701018@csu.edu.cn

1 School of Mechanical and Electrical Engineering, Central South University, Changsha 410083, China

2 Shenzhen Research Institute of Central South University, Shenzhen 518000, China

3 State Key Laboratory of Deep Sea Mineral Researches Development and Utilization Technology, Changsha 410012, China

Fig. 1 Pipe-lifting system of deep-sea mining. (1)Mining vessel. (2) lifting motor pump. (3) Riser pipe. (4) Middle bin. (5) Soft pipe. (6) Collector

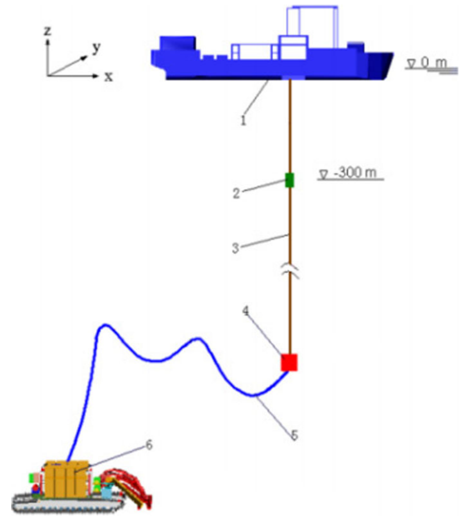

1-Mining vessel, 2-Lifting motor pump,3-Riser pipe, 4-Middle bin,5-Soft pipe,6-Collector

technology, some new technologies were applied to measure multiphase flow, such as fiber technology, ultrasonic technology, particle image technology, laser technology, and process tomography technology (Pu et al. 2006; Du et al. 2015; Zhang et al. 2014). Industrial multiphase flow parameter measurement requires non-invasion, high-reliability, high-precision, real-time measurement; many scholars had done a lot of creative work in these areas. Li et al. (2014) proposed an improved EEMD filtering method for multiphase flow signal. Experiments revealed that this method could improve the accuracy of multiphase flow measurement. Wang et al. (2014) proposed a measurement method of oil and gas multiphase flow that combined with the relevant flow measurement method and electromagnetic flow measurement method. Zheng et al. (2008a) achieved gas-liquid two-phase flow measurement by applying conductivity sensor combined with turbine flowmeter. Yang et al. (2017) developed a droplet-capable conductivity probe for the measurement of liquid-dispersed two-phase flow. Xiuzhong and Hideo (2014) proposed a newly developed complete four-sensor probe signal processing algorithm for local instantaneous 3-dimensional bubble velocity vector. Khasani et al. (2017) studied on the transient behaviors of two-phase flow in a geothermal production well for a short period of continuous measurement. Wang et al. (2016) proposed a method for measuring gas-liquid two-phase flow based on near-infrared spectroscopy. He et al. (2016) designed an on-line measuring device to measure the gas-liquid flow rate in wet gas by using a V-shaped conical throttle device. Fang et al. (2018) proposed two-phase fluid phase content measurements based on near-infrared absorption and decay techniques.

In recent years, capacitively coupled contactless conductivity detection (C^4D) technology has been more and more concerned by the fluid parameter measurement field, as it can avoid effectively electrode corrosion and polarization issues in traditional conductance detection. Ji et al. (2014) developed a C^4D sensor for millimeter pipeline fluid measurement in the industrial field. Zheng et al. (2008b) proposed a C^4D measurement method based on parallel resonance and applied this method successfully to the measurement of

Fig. 2 Collector for deep-sea mining. (1) Left roller. (2) Right roller. (3) Collecting cover. (4) Pump. (5) Rocker arm. (6) Ore trolley. (7) Soft pipe

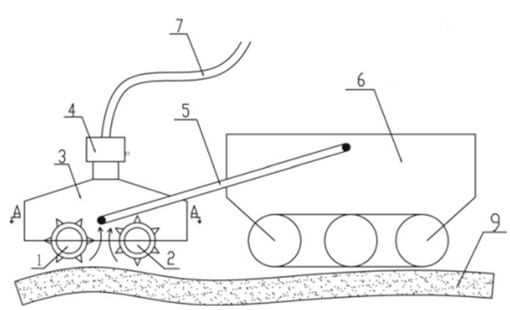

1-Left roller, 2-Right roller, 3-Collecting cover, 4- pump,5-Rocker arm,6-Ore trolley, 7-Soft pipe

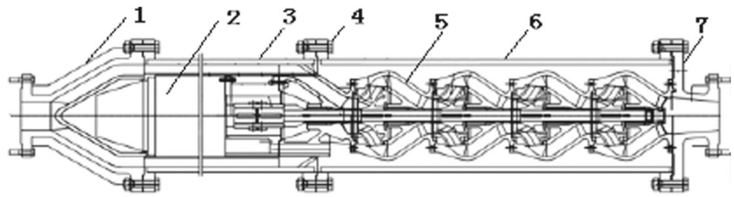

1-Flange of Suction,2-Motor,3-Annular channel,4-Nut and bolt,5-Multistage pump,6-Pump barrel ,7-Flange of spit out.

Fig. 3 Structure of lifting motor pump. (1) Flange of suction. (2) Motor, (3) Annular channel. (4) Nut and bolt. (5) multistage pump. (6) Pump barrel. (7) Flange of spit out

microparticles in fluid. Huang et al. (2009, 2012) proposed a C4D measurement method based on the impedance cancellation principle and designed a C4D sensor with a single shield.

Achievements mentioned previously were mainly for the measurement of gas-liquid two-phase flow in small pipelines. These achievements and methods had more or less a certain reference to the measurement of solid-liquid two-phase flow parameters. But fluid transported in pipeline-lifting system of deep-sea mining is a solid-liquid two-phase flow consisting of polymetallic nodule particles and sea water, its mechanism and state are significantly different from the gas-liquid two-phase flow, so it is necessary to further study the measurement method of solid-liquid two-phase flow in pipeline-lifting system of deep-sea mining. In this study, the objective was to meet the requirements of the parameter measurement of two-phase flow in pipeline-lifting system of deep-sea mining. Therefore, a differential C4D method was used to measure solid-liquid two-phase flow parameters in the proposed mineral pipeline transportation. The conclusion has some reference significance to improve the accuracy of measurement for multiphase flow transporting in pipeline.

Materials and Methods

Composition and Working Principle of C4D for Fluid in a Pipeline

Construction and equivalent of C4D sensor are shown in Fig. 4. It consists of five main components: insulation pipe, AC excitation signal source, driving electrode, detecting electrode, and signal processing section. Electrodes of driving and detecting were two ring metal electrodes, which were closed to the outer wall of the insulation pipe. So the metal electrodes, insulated pipe, and conductive fluid formed an AC signal path. When the excitation signal with a certain frequency was applied to the excitation electrode, the response signal associated with the conductivity of the fluid could be detected at the detecting electrode.

In the equivalent of C4D sensor, R_S is the equivalent resistance of measured fluid. C_1 and C_2 are the capacitors formed by two metal electrodes coupling with conductive liquid. C_0 is the stray capacitor formed by two metal electrodes with coupling through air. It is detrimental to the conductance measurement and could be eliminated by adding a ground shield between the two metal electrodes (Pumera 2007) as shown in Fig. 4. The total impedance of C4D is expressed as follows:

$$Z = R + jX_C = \frac{R_S C_S^2 \omega^2 - j\left[\omega(C_S + C_0) + R_S^2 C_0 C_S^2 \omega^3\right]}{(R_S C_0 C_S \omega^2) + \left[\omega(C_S + C_0)\right]^2} \quad (1)$$

where R and X_C are the real and imaginary parts of the capacitively coupled contactless reactance, respectively; $\omega = 2\pi f$, f is the frequency of the excitation signal; C_S is the series value of the coupling capacitors C_1 and C_2. In conductance measurement circuit, the equivalent resistance of fluid R_S is a useful signal, but coupling capacitors C_1 and C_2 are unfavorable background signals. Due to the large size of the pipeline for transporting solid-liquid two-phase flow, therefore, the equivalent resistance of fluid R_S was small and the

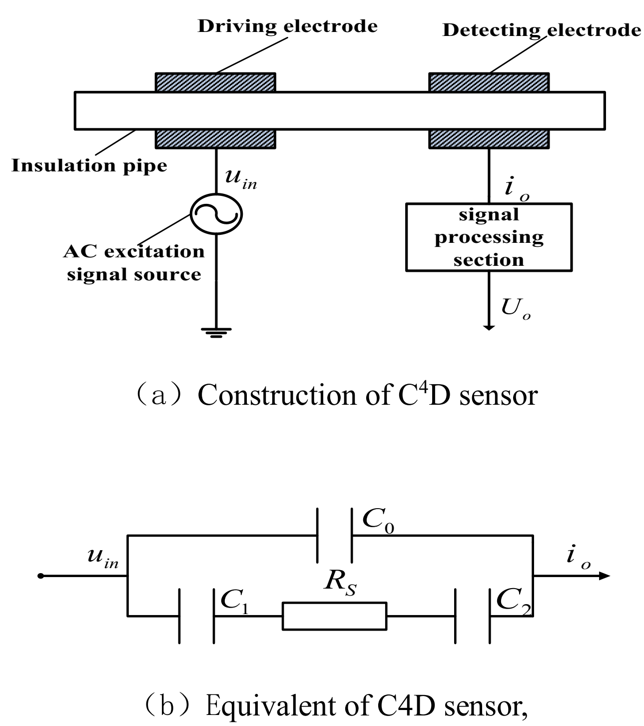

Fig. 4 Construction and equivalent of C4D sensor. **a** Construction of C4D sensor. **b** Equivalent of C4D sensor

capacitances of coupling capacitor C_1 and C_2 were large, resulting in a low signal-to-noise ratio of the measurement device and low measurement sensitivity (Laugere et al. 2002).

A New Structure of Serial-Resonant C[4]D Sensor Introducing Virtual Inductor

In order to improve the sensitivity of conductivity measurement, we can use series resonant to eliminate the effects of coupling capacitors and use the metal electrode shield to eliminate the effects of stray capacitors. In serial-resonant C[4]D sensor, the resonant frequency is determined by the coupling capacitors and inductor. When the condition of fluid in the pipeline is determined, therefore, the coupling capacitance is constant. If the actual inductance is used in the sensor, the range of resonant frequencies is limited. Since the virtual inductance has the advantages of adjustable inductance and low resistance, if we use it instead of the actual inductance in the serial-resonant C[4]D sensor, it can easily adjust the range of resonant frequency and reduce the requirements of sensor to excitation signal source. In this paper, we proposed an improved virtual inductor on the basis of traditional virtual inductor with grounded structure, it can overcome the defect of one end of the grounded virtual inductor that must be grounded. So this virtual inductor can be integrated into a separate module, which can be directly applied to the C[4]D sensor. The circuit of the improved virtual inductor is shown in Fig. 5.

The analysis of the circuit in Fig. 5 shows that:

$$\frac{(u_1 - u_m)}{R_4} = \frac{(u_m - u_2)}{R_5} = \frac{V_{\text{out2}} - u_1}{R_6} \tag{2}$$

$$\frac{(u_1 - V_{\text{out1}})}{\frac{R_2}{1 + j\omega c R_2}} = \frac{V_{\text{out2}} - u_1}{R_3} \tag{3}$$

where u_1 and u_2 are the input voltage signal and the output voltage signal of the virtual inductive circuit respectively, V_{out1} and V_{out2} are the output signals of the operational amplifiers A_1 and A_2, and u_{m} represents the voltage value between the resistors R_4 and R_5.

By combining Eqs. (2) and (3), the input current i_1 of the entire circuit is expressed as follows:

$$\begin{aligned} i_1 &= \frac{u_1 - V_{\text{out1}}}{R_1} = \frac{(V_{\text{OUT2}} - u_1) R_2}{R_1 R_3 (1 + j\omega c R_2)} \\ &= \frac{(u_1 - u_m) R_2 R_6}{R_1 R_3 R_4 (1 + j\omega c R_2)} \end{aligned} \tag{4}$$

Similarly, it can be seen that the output current i_2 of the entire circuit is:

$$i_2 = \frac{(u_m - u_2) R_7 R_9}{R_5 R_8 R_{10} (1 + j\omega c R_9)} \tag{5}$$

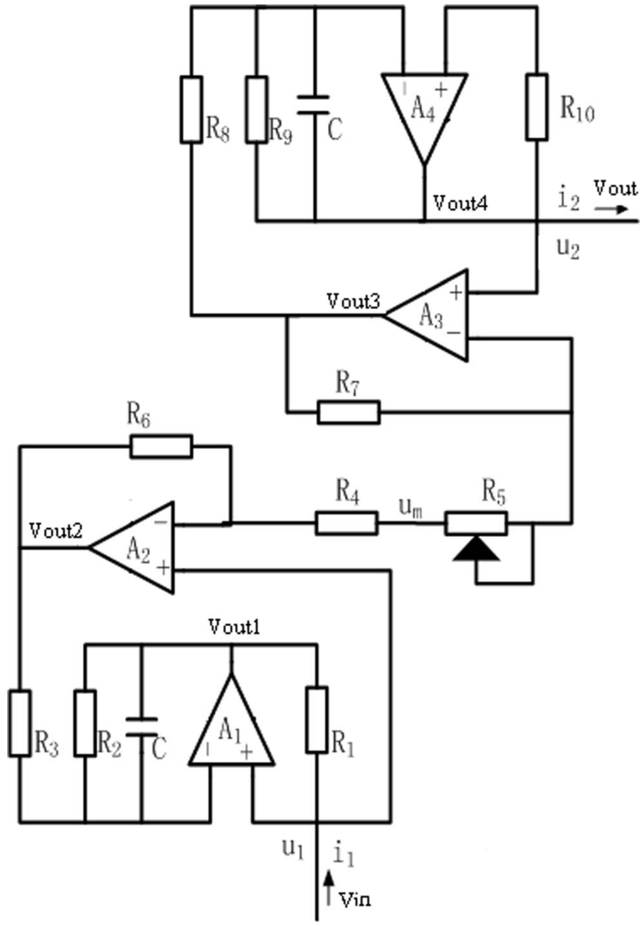

Fig. 5 Circuit of virtual inductance

In order to make the virtual inductance be applied to the C[4]D sensor as a separate module, it needs to satisfy $i_1 = i_2$, which is:

$$\frac{(u_1 - u_m) R_2 R_6}{R_1 R_3 R_4 (1 + j\omega c R_2)} = \frac{(u_m - u_2) R_7 R_9}{R_5 R_8 R_{10} (1 + j\omega c R_9)} \tag{6}$$

It is known from the Eq. (2):

$$\frac{(u_1 - u_m)}{R_4} = \frac{(u_m - u_2)}{R_5} \tag{7}$$

By substituting Eq. (7) into Eq. (6), Eq. (6) can be reduced as follows:

$$\frac{R_2 R_6}{R_1 R_3 (1 + j\omega c R_2)} = \frac{R_7 R_9}{R_8 R_{10} (1 + j\omega c R_9)} \tag{8}$$

In order to conveniently calculate the above equation, the resistance in the circuit can be selected according to the following rules:

$$\frac{R_2}{R_9} = \frac{R_7}{R_6} \tag{9}$$

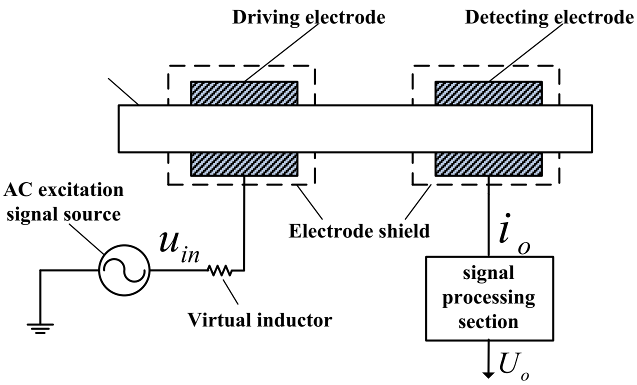

Fig. 6 Serial-resonant C[4]D sensor based on virtual inductance

$$\frac{R_1}{R_{10}} = \frac{R_8}{R_3} \tag{10}$$

By calculating Eq. (4)~Eq. (10), the impedance of the virtual inductance Z_v is as follows:

$$\begin{aligned} Z_v &= \frac{V_i - V_O}{I_{in}} = \frac{u_1 - u_2}{i_1} \\ &= \frac{R_1R_3(R_4+R_5)}{R_2R_6} + j\omega c \frac{R_1R_3(R_4+R_5)}{R_6} \\ &= R_v + j\omega L_v \end{aligned} \tag{11}$$

Eq. (11) indicates that the circuit of the virtual inductor can be equivalent to the resistance R_v and the inductor L_v in series. R_v and L_v are calculated as follows:

$$R_v = \frac{R_1R_3(R_4+R_5)}{R_2R_6} \tag{12}$$

$$L_v = c\frac{R_1R_3(R_4+R_5)}{R_6} \tag{13}$$

Eq. (13) indicates that in the circuit of the virtual inductor shown in Fig. 5, even if the other circuit parameters remain unchanged, the value of inductance can be changed by adjusting the slide resistance R_5.

The serial-resonant C[4]D sensor introducing virtual inductor proposed in this paper is shown in Fig. 6; its equivalent circuit is shown in Fig. 7, where C_1 and C_2 are the capacitors formed by two metal electrodes coupling with conductive liquid. R_S is the resistance of the conductive fluid and R_V and L_V are the equivalent resistance and inductance of the virtual inductor circuit, respectively. So the total impedance of the serial-resonant C[4]D sensor z can be expressed as follows:

$$Z = R_v + R_S + j2\pi f L_v - \frac{j(C_1+C_2)}{2\pi f C_1 C_2} \tag{14}$$

where f is the frequency of the excitation signal. When the circuit is resonant, the capacitive reactance generated by the coupling capacitors C_1 and C_2 is offset against the inductive reactance generated by the inductor. At this time, the total impedance of the sensor is $Z_0 = R_V + R_S$. The resonance frequency of the circuit f_0 is calculated as follows:

$$f_0 = \frac{1}{2\pi}\sqrt{\frac{C_1+C_2}{L_v C_1 C_2}} \tag{15}$$

Measurement of Two-Phase Flow in Slurry Pipeline Based on Differential C[4]D

The structure of the measuring device for two-phase flow in a slurry pipeline based on differential C[4]D sensor is shown in Fig. 8. It consists of two serial-resonant C[4]D sensors, while it has only three electrodes. The center electrode was shared by the two C[4]D sensors, as driving electrode, which was applied the excitation signal with a certain frequency at the time of operation. The upper and lower of the measuring device are detecting electrodes. The differential signal between the two detecting electrodes was amplified and then filtered out the high-frequency noise components, so the output signal of the measuring device represents the voltage difference

Fig. 7 Equivalent of serial-resonant C[4]D sensor based on virtual inductance

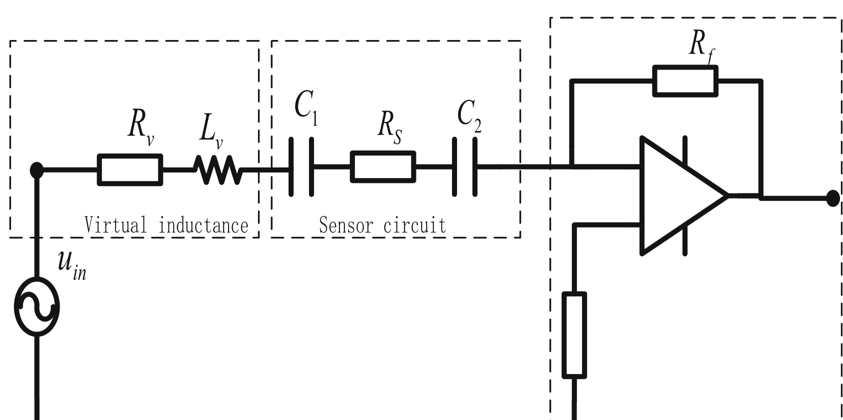

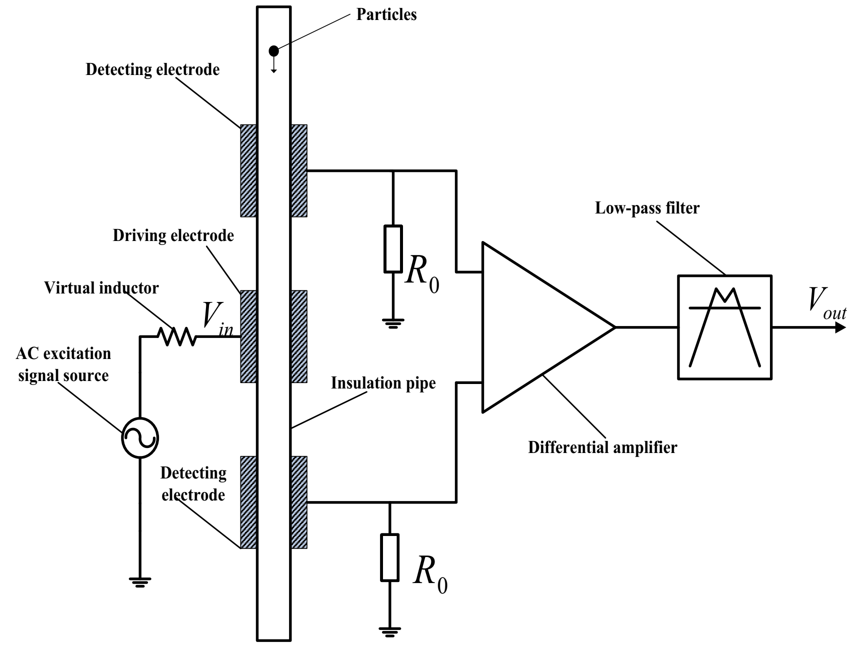

Fig. 8 Structure of measuring device for two-phase flow in slurry pipeline based on C^4D differential sensor

between the two C^4D sensor output signals. The equivalent of the differential C^4D circuit is shown in Fig. 9. The differential signal between the two C^4D sensors $\Delta u = U_{\text{out1}} - U_{\text{out2}}$ was amplified by the measuring device, but the common mode signal such as noise in fluid motion was offset. So this construction could reduce the influence of the fluid noise on the measurement.

The fluid transported in slurry pipeline for deep-sea mining is a solid-liquid two-phase flow that is composed of polymetallic nodules and seawater. Because the conductivity of seawater is high, usually (3~5) s/m, so in the conductance detection process; the total impedance between electrodes is small. In the equivalent circuit, the capacitance depended primarily on the stray capacitor C_0 between the pairs of metal electrodes. When the metal electrodes were fixed, the stray capacitor C_0 between electrodes was constant and could even use a shield to eliminate the influence of stray capacitor C_0. Therefore, when mineral particles move in the pipeline, the conductivity of the fluid mainly depended on the fluid change in the cross section of the pipeline. The equivalent of solid-liquid two-phase flow based on C^4D is shown in Fig. 10. Assume that polymetallic nodule particles were equivalent to spherical particles of diameter H_2, and the internal pipeline surrounded by electrodes was divided into three sections of length H_1, H_2, and H_3. The first section H_1 and the last section H_3 contain only homogeneous fluids such as seawater, while the middle section H_2 contains a mixture of seawater and polymetallic nodules. The corresponding electrode coupling capacitor was also divided into three parts such as C_{11}, C_{12}, and C_{13}. So the total impedance of the equivalent circuit Z is expressed as follows:

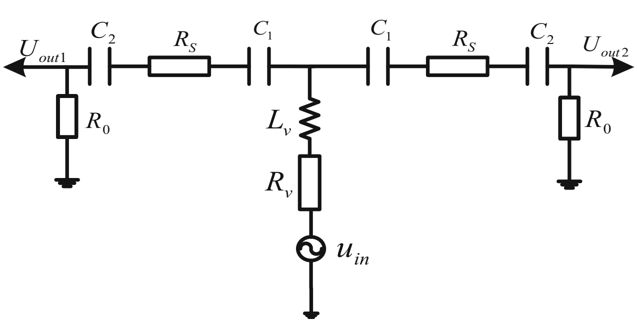

Fig. 9 Equivalent of measuring device for two-phase flow in slurry pipeline based on C^4D differential sensor

$$Z = R_v + R_S + R_{S3} + R_0 + j\omega L_v + \frac{1}{j\omega C_2} + \frac{X}{Y} \tag{16}$$

$$X = j\text{–}[(C_{S1} + R_{S2})C_{11} + C_{12}R_{S2}] - jC_{11}C_{12}R_{S1}R_{S2}\omega^2 \tag{17}$$

$$Y = C_{11}C_{12}C_{13}R_{S1}R_{S2}\omega^3 - \omega(C_{11} + C_{12} + C_{13}) - j\omega^2[(C_{12} + C_{13})C_{11}R_{S1} + (C_{11} + C_{12})C_{13}R_{S2}] \tag{18}$$

Among them, the resistance and capacitance are as follows:

$$R_{S1} = \rho\frac{4H_1}{\pi D^2} \tag{19}$$

$$R_{S2} = \rho\frac{4H_2}{\pi\left(D^2 - H_2^2\right)} \tag{20}$$

$$R_{S3} = \rho\frac{4H_3}{\pi D^2} \tag{21}$$

$$C_{11} = \frac{H_1}{H}C_2 \tag{22}$$

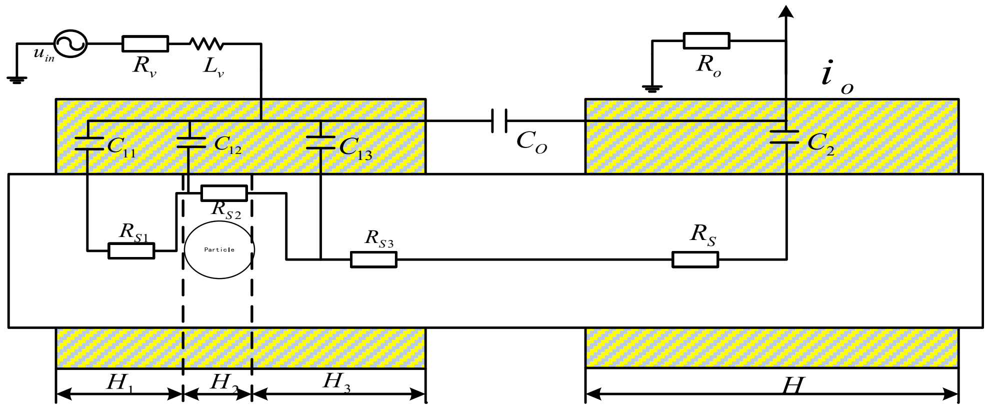

Fig. 10 Equivalent of solid-liquid two-phase flow based on C[4]D

$$C_{12} = \frac{H_2}{H} C_2 \tag{23}$$

$$C_{13} = \frac{H_3}{H} C_2 \tag{24}$$

where D is the diameter of the measured pipe, ρ is the resistivity of seawater, and ω = 2π*f*, *f* represents the frequency of the excitation signal.

Fig. 11 Experimental device of measurement for two-phase flow in slurry pipeline based on C[4]D

Table 1 Geometrical parameters of the measuring device

Pipe outside diameter/mm	Pipe inside diameter/mm	Electrode length/mm	Electrode spacing/mm
200	180	90	15

Measurement Experiment

The experimental device of the measurement for two-phase flow in a slurry pipeline based on the differential C^4D is shown in Fig. 11. It consisted mainly of the conveying pipeline, mining ship simulation platform, control cabinet, differential C^4D sensor, and data acquisition system. The geometric parameter of the measuring device based on the differential C^4D is shown in Table 1. In the test process, the excitation signal with a peak value of 8 V and a frequency of 120 kHz was first applied on the center electrode of the differential C^4D sensor, and then, its virtual inductance was adjusted until the circuit resonates. At the same time, the output signal of the differential C^4D was collected by the data acquisition card to the computer for data processing, then, the parameters of the two-phase flow in the slurry pipeline could be obtained by computer processing. The control cabinet could adjust the pump speed through a frequency changer and change the velocity of the two-phase flow in the slurry pipeline.

Conductive fluid used in the experiment is KCl solution with salinity ranging from 0 to 4%. The nodules are artificial manganese nodules with the nodule density of 2000 kg/m^3, as shown in Fig. 12. The manganese nodules of different particle sizes were mixed with different salinity fluids in the middle bin, then the mixture was pumped into the slurry pipeline, as shown in Fig. 13.

Results and Discussion

The output voltage signal of the measuring device when nodules passed through electrodes is shown in Fig. 14. There were no spikes in the output signal, indicating that the use of the differential structure in C^4D can effectively restrain the influence of fluid noise. The two positive and negative peaks of the output voltage signal represent the time when the polymetallic nodules reach the geometric center of the two electrodes, respectively. According to the distance L between the geometric center of two electrodes and the time difference ΔT between the positive and negative peaks of the output voltage, the particle's velocity V of two-phase flow in the pipeline can be calculated as follows:

$$V = \frac{L}{\Delta T} \tag{25}$$

As shown in Fig. 14, the two points A and B are the geometric center of the upper and lower electrodes of the measuring device, respectively. The distance between them is 210 mm. When the measuring device outputted a negative peak, that is the time the nodules passed through point A, which was 218 ms. When the measuring device outputted a positive peak, that is the time the nodules passed through point B, which was 276 ms. So, it could be calculated that the particle velocity of two-phase flow in pipeline is 3.62 m/s. This result is in good agreement with the speed of 3.8 m/s calculated by the trajectory of solid particles collected by a high-speed camera, as shown in Fig. 15.

In fact, nodules in the slurry transported by deep-sea pipelines consist of a variety of particles. On the whole, the volume fraction of the nodules is relatively low, generally less than 8% (Tang et al. 2015). Therefore, when multiple nodules passed through the electrode of the measuring device at the same time, the multiple nodules can be equivalent to a larger size nodule according to the actual flow of the fluid in the cross section of the pipelines.

The output voltage of the measuring device was related to the salinity of two-phase flow and the particle size of polymetallic nodules. In fluids with different salinity, the output voltage signal of the measuring device when nodules with different sizes passed through the electrode is shown in Fig. 16. The results indicated that the amplitude of the output

Fig. 12 Simulated manganese nodules of different particle sizes. **a** 5 mm. **b** 10 mm. **c** 20 mm

（a）5mm (b) 10mm (c) 20mm

Fig. 13 Mixture of nodules and conductive fluids. **a** The maximum particle size of a single nodule = 10 mm, fluid salinity 3.5%. **b** The maximum particle size of a single nodule = 20 mm, fluid salinity 1.5%

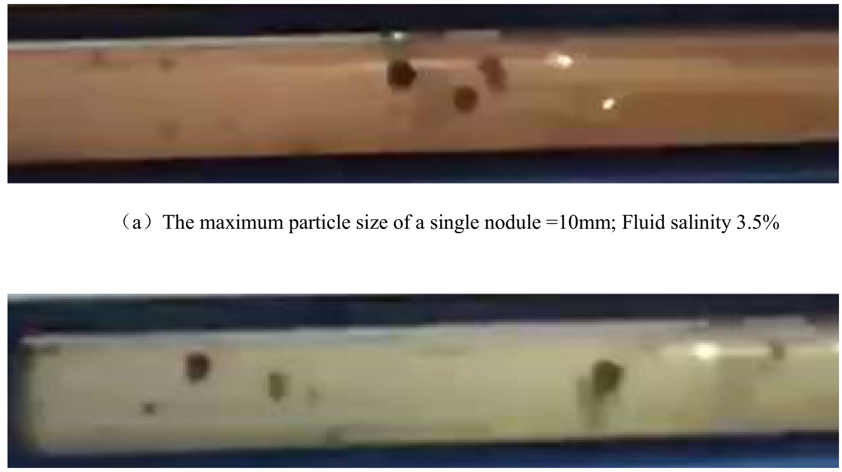

（a）The maximum particle size of a single nodule =10mm; Fluid salinity 3.5%

（b）The maximum particle size of a single nodule =20mm; Fluid salinity 1.5%

voltage signal of the measuring device increases with the increase of the size of the polymetallic nodules in the pipeline. When the salinity of the KCl solution, as a conductive fluid in the pipeline, is at an average salinity of seawater 3.5%, the diameter of polymetallic nodules increased from 0 to 25 mm, and the amplitude of the output voltage signal increased from 0 to 87 mv. In addition, the amplitude of the output voltage signal decreased along with the increased salinity of two-phase flow. When the diameter of the polymetallic nodules is 20 mm, the salinity of two-phase flow increased from 1.5 to 3.8%, and the amplitude of the output voltage signal decreased from 150 to 47 mv.

In addition, the output voltage of the measuring device was related to the slurry density. Since the slurry transported by deep-sea pipelines is a mixture of nodules and seawater, the relationship between the mixture density and the volume concentration of the manganese nodules is shown in Fig. 17. When the volume concentration of the manganese nodules increased from 0 to 10%, the density of the mixture increased from 1037 to 1133 kg/m^3.

Fig. 14 Output voltage signal of the device when particles pass through electrodes

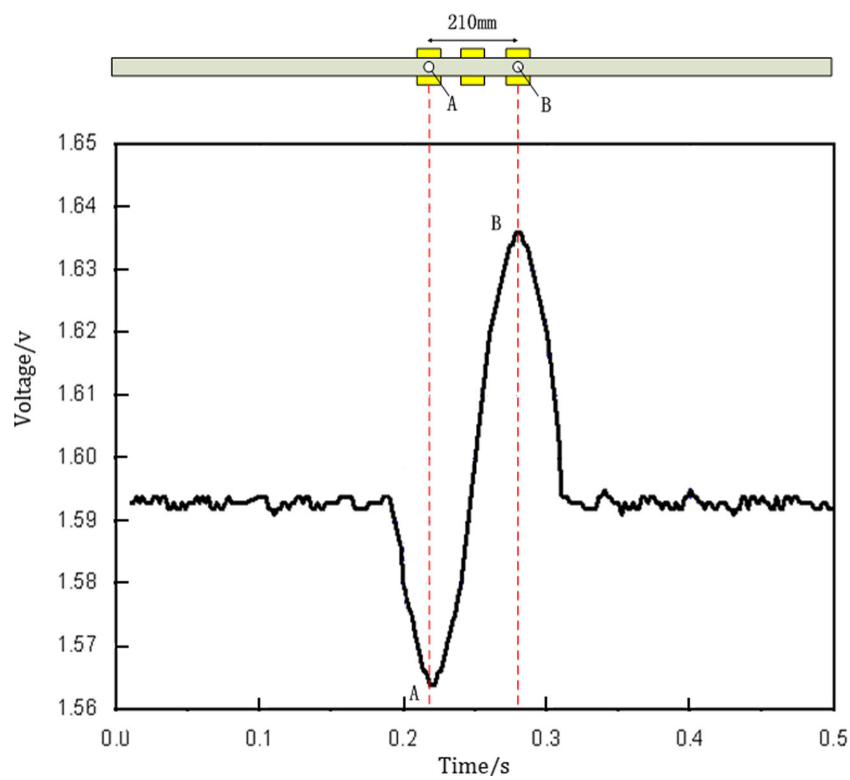

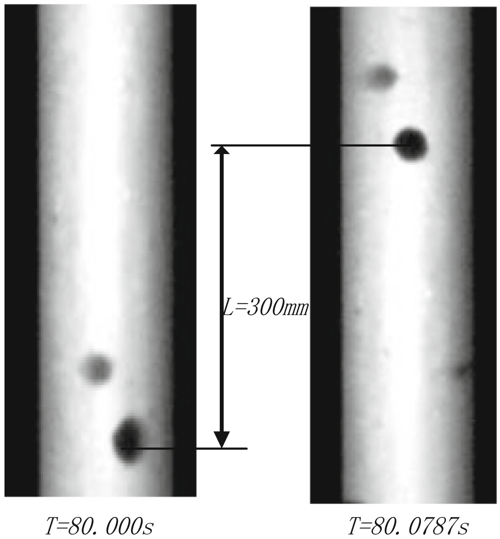

Fig. 15 Trajectory of solid particles collected by the high-speed camera

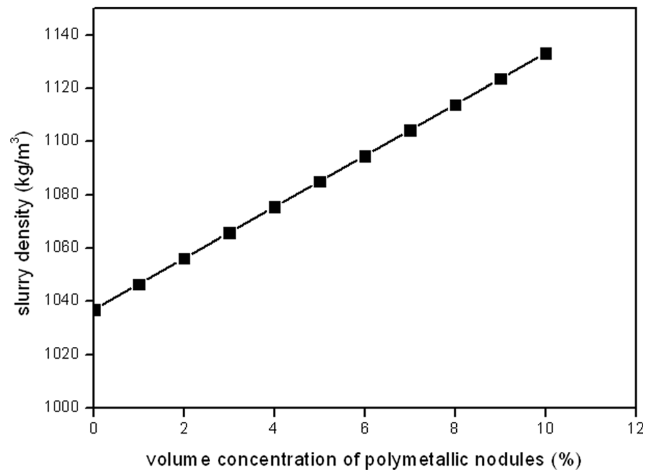

Fig. 17 Relationship between the mixture density and the volume concentration of manganese nodules

In a slurry with a constant salinity of 3.5%, but with different densities, when the manganese nodules with a maximum particle size of 20 mm passed through the electrodes, the output voltage amplitude of the measuring device increased as shown in Fig. 18. When slurry density increased from 1037 to 1133 kg/m^3, the output voltage amplitude of the measuring device increased from 61 to 69 mv, indicating that slurry density had a certain degree of influence on electrical conductivity.

Through the repeated measurement experiment of two-phase flow in a slurry pipeline, the results showed that the measuring method proposed in this paper had a high accuracy. The experimental results of a typical velocity measuring for two-phase flow are shown in Fig. 19. The results demonstrated that the relative error of the two-phase flow velocity was 5.2% and most of the relative error was less than 5% when the KCl solution was 3.5% and the particle size of the polymetallic nodules was 20 mm. Therefore, the measuring method for two-phase flow in a slurry pipeline proposed in this paper is effective.

Conclusion

Through analysis, the C^{4}D with three-electrode differential structure can effectively reduce the influence of fluid noise on the measurement parameters. The serial-resonant C^{4}D sensor incorporating a virtual inductance has the advantages of adjustable inductance and small internal resistance, thereby reducing the requirements of C^{4}D sensor to excitation signal source. The output voltage signal of differential C^{4}D is related to the salinity of two-phase flow and the particle size and volume concentration of polymetallic nodule. When the conductive fluid in the pipeline is at the average salinity of

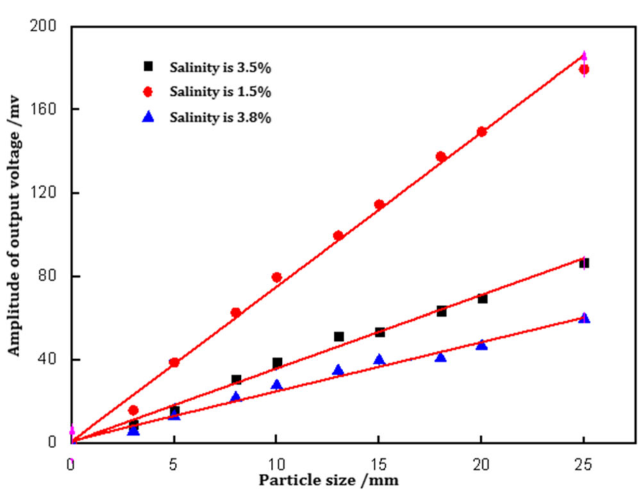

Fig. 16 Relationship between output voltage and particle size at different salinity of fluid

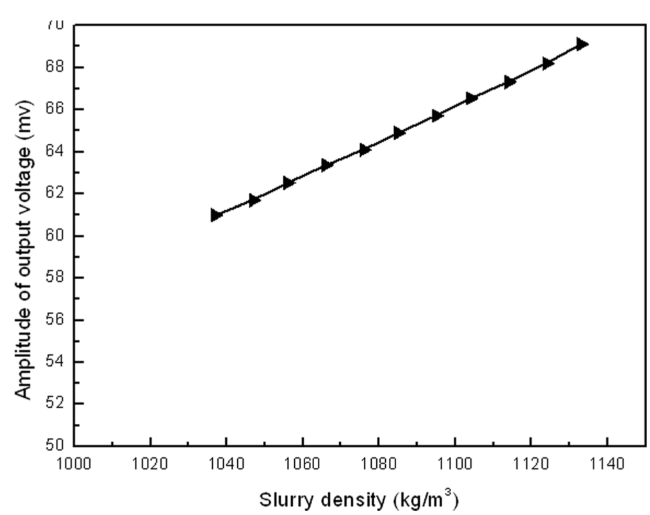

Fig. 18 Relationship between output voltage and slurry density

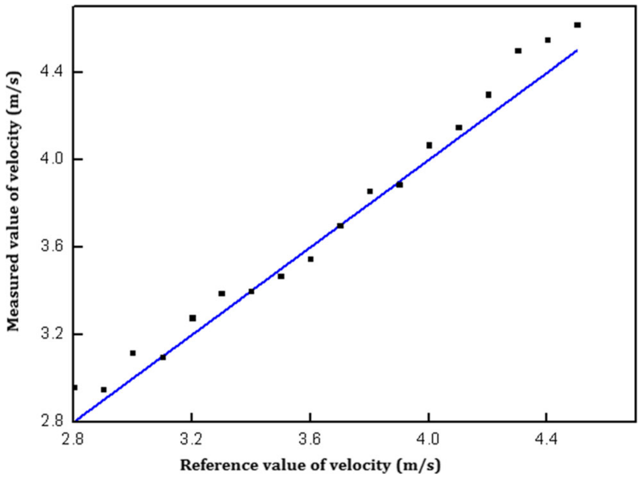

Fig. 19 Typical group of velocity measurement results of two-phase flow

seawater 3.5%, the amplitude of the output voltage signal of the differential C^4D sensor increases along with the increased particle size of polymetallic nodules in pipeline. When the particle size is constant, the amplitude of the output voltage signal decreases along with the increased salinity of two-phase flow. In the differential C^4D-based measurement process, according to the distance between two electrodes and the time difference between the positive and negative peaks of the output voltage, the particle's velocity of two-phase flow in the pipeline can be calculated. The measurement accuracy of the differential C^4D is high, and the maximum relative error of flow velocity measurement in the experiment is 5.2%. The proposed measurement method of two-phase flow in slurry pipeline based on differential C^4D is effective.

Funding Information The authors would like to thank the following foundations:

1. National Key Research & Development project of China (2016YFC0304103)
2. Research project of Shenzhen Science and Technology innovation (JCYJ20150929102555935)
3. Major support Plan Project of Shenzhen (HYZDFC20140801010002)

References

Du X, Sun N, Wang M (2015) Analysis of gas-liquid two phase flow velocity field under varying aeration rate based on PIV measurement technique. J Hydraul Eng 11:1371–1377

Fang L, Lu X, Tian J et al (2018) Dual-parameter measurement based on near infrared and differential pressure technique in gas-liquid two-phase flow. China Meas Test 44(1):21–26

He DE, Bai BF, Zhang J et al (2016) Online measurement of gas and liquid flow rate in wet gas through one V-Cone throttle device. Exp Thermal Fluid Sci 75:129–136

Huang ZY, Jiang WW, Zhou XM, Wang BL, Ji HF, Li HQ (2009) A new method of capacitively coupled contactless conductivity detection based on series resonance. Sensors Actuators B Chem 143:239–245

Huang ZY, Long J, Xu W, Ji HF, Wang B, Li HQ (2012) Design of capacitively coupled contactless conductivity detection sensor. Flow Meas Instrum 27:67–70

Ji H, Li Z, Wang B et al (2014) Design and implementation of an industrial C4D sensor for conductivity detection. Sensors Actuators A Phys 213:1–8

Khasani S, Jalilinasrabady T, Tanaka H, Fujii R, Itoi (2017) The study on transient behaviors of two-phase flow in a geothermal production well for a short period of continuous measurement. Exp Thermal Fluid Sci 84:10–17

Laugere F, Lubking GW, Bastemeijer J, Vellekoop MJ (2002) Design of an electronic interface for capacitive coupled four-electrode conductivity detection in capillary electrophoresis microchip. Sensors Actuators B 83:104–108

Li L, Dang R, Fan Y (2014) Modified EEMD de-noising method and its application in multiphase flow measurement. Chin J Sci Instrum 10: 2365–2371

Liu S, Liu C, Dai Y (2014) Status and progress on researches and developments of deep ocean mining equipments. J Mech Eng 02:8–18

Liu S, Hu J, Zhang R et al (2016) Development of mining technology and equipment for seafloor massive sulfide deposits. J Mech Eng 29(5): 863–870

Pu S, Lu Z, Pu X et al (2006) Application of interfere metric laser imaging technique for spray spatial diameter distribution measurement. J Zhejiang Univ (Eng Sci) 10:1801–1804

Pumera M (2007) Contactless conductivity detection for micro fluidics: designs and applications. Talanta 74:358–364

Tang D, Yang N, Gong D, Xiao H et al (2015) Experimental study of manganese nodules pump in deep-sea mining. Ocean Eng 33(4): 101–107

Wang Y, Kong L, Liu X (2014) Detection electrode distance study of electromagnetic correlation method flow measurement sensor. Tran Micro Techno 07:49–52

Wang C, Zhao N, Fang LD (2016) Void fraction measurement using NIR technology for horizontal wet-gas annular flow. Exp Thermal Fluid Sci 76:98–108

Xiao Y, Yang L, Li CAO et al (2014) Distribution of marine mineral resource and advances of deep-sea lifting pump technology. J Drain Irrig Mach Eng 04:319–326

Xiuzhong S, Hideo N (2014) Spherical-bubble-based four-sensor probe signal processing algorithm for two-phase flow measurement. Int J Multiphase Flow 60:11–29

Yang L, Xiaohong Y, Qingzi Z, Peng J, Mamoru I, Buchanan JR (2017) Development of the droplet-capable conductivity probe for measurement of liquid-dispersed two-phase flow. Int J Multiphase Flow 88:238–250

Zhang Y, Dong F, Xu C et al (2014) Ultrasonic method for gas-liquid two phase flow void fraction measurement. Chin J Sci Instrum 09:2094–2101

Zheng GB, Jin ND, Jia XH, Lv PJ, Liu XB (2008a) Gas-liquid two phase flow measurement method based on combination instrument of turbine flow meter and conductance sensor. Int J Multiphase Flow 34(11):1031–1047

Zheng SY, Nandra MS, Shih CY, Li W, Tai YC (2008b) Resonance impedance sensing of human blood cells. Sensors Actuators A: Phys 145:29–36